This is an *Accepted Manuscript*, which has been through the Royal Society of Chemistry peer review process and has been accepted for publication.

Accepted Manuscripts are published online shortly after acceptance, before technical editing, formatting and proof reading. Using this free service, authors can make their results available to the community, in citable form, before we publish the edited article. We will replace this *Accepted Manuscript* with the edited and formatted *Advance Article* as soon as it is available.

You can find more information about *Accepted Manuscripts* in the **Information for Authors**.

ChemComm

COMMUNICATION

A facile method for the synthesis of $Li_{0.3}La_{0.57}TiO_3$ solid state electrolyte

Qifeng Zhang[a], Nick Schmidt[a], Jolin Lan[a], Whungwhoe Kim[b], and Guozhong Cao[a,*]

We report a facile method for the synthesis of $Li_{0.3}La_{0.57}TiO_3$ by forming a coagulated precursor solution which contains Li^+, La^{3+}, and TiO_2 nanoparticles mixed highly homogeneously. The grain and overall conductivities of the synthesized $Li_{0.3}La_{0.57}TiO_3$ are comparable to the values in literature for the material prepared by other methods.

There is an increasing demand for solid state electrolytes for use in lithium batteries to replace the currently widely used liquid electrolytes in recent years. Compared to liquid electrolytes, solid state electrolytes possess advantage in providing lithium batteries with much safer operation[1, 2] and making the manufacture easier thus resulting in significant reduction of battery cost. In some cases, to use solid state electrolytes has become an essential requirement. For instance, in lithium ion batteries, solid state electrolytes have been expected to replace the liquid electrolytes with the consideration of blocking the growth of lithium dendrites through charge/discharge cycles; such lithium dendrites may connect the anode and cathode ultimately causing an internal short circuit of the battery.[3-5] Solid state electrolytes are also desired for lithium air battery applications, where they serve as a membrane to separate the organic electrolyte from the aqueous electrolyte. The organic electrolyte is adopted to protect the lithium anode from reacting with water, while the aqueous electrolyte is used to facilitate the dissolution of lithium oxides (particularly lithium peroxide, Li_2O_2) formed at the cathode during discharge, which are insoluble in organic electrolytes and may therefore cause either passivation or pore blocking of the cathode, which is typically made of porous carbon.[6, 7] In addition, solid state electrolytes are also an integral component for the construction of lithium batteries to operate at temperatures below -10 °C or above 60 °C, which are the temperature limit for most liquid electrolytes.[8]

Many efforts have been made to develop solid state electrolyte, including the use of both inorganic materials and polymers.[9-11] The advantage of polymer-based electrolytes is that they are bendable and therefore can work with flexible substrates and are compatible with the roll-to-roll technology. However, the polymer-based electrolytes suffer from a poor chemical stability especially when taking the heat generation which occurs during the battery operation into account. Compared to polymer-based electrolytes, inorganic electrolytes demonstrate much better chemical stability and, more importantly, present significantly higher lithium ionic conductivity, typically on the orders of 10^{-5}-10^{-3} S/cm, compared to 10^{-8}-10^{-6} S/cm for most polymer electrolytes.[12-14] Among the existing inorganic electrolytes, lithium lanthanum titanate (LLTO) has been identified as the most promising one in view of its high lithium ionic conductivity, typically on the orders of 10^{-4}-10^{-3} S/cm (for single crystalline grains).[10, 15-18] Such a conductivity level is averagely higher than that for Na super-ionic conductor structure phosphate salts – which is another inorganic solid state electrolyte with great potential,[10, 19-21] and is apparently 1~2 orders of magnitude higher than the conductivities for other inorganic solid electrolytes, such as 10^{-6}-10^{-4} S/cm for garnet structure materials,[22-24] and 10^{-5}-10^{-3} S/cm for Li_2S-based oxysulfide glasses.[25, 26] In addition to the advantage of having high conductivity, good thermal stability and the use of nontoxic elements are also amongst the merits of lithium lanthanum titanate over other inorganic solid state electrolytes.

Lithium lanthanum titanate is a ceramic material possessing ABO_3 perovskite structure, in which A represents Li and La, and B represents Ti, forming a lithium-lanthanum-titanium oxide with the formula of $Li_{3x}La_{2/3-x}TiO_3$ ($0.21{\leq}3x{\leq}0.50$). In lithium lanthanum titanate, the migration of lithium ions is based on a hopping process, through which the lithium ions move in a three-dimensional network of vacancy defects located at A sites. Lithium ion conduction within lithium lanthanum titanate is very sensitive to the concentration of lithium, in other words, the stoichiometric ratios of the Li^+ to La^{3+} and TiO_3^{2+}. It has been found that $Li_{3x}La_{2/3-x}TiO_3$ in the case of x=0.1, i.e., $Li_{0.3}La_{0.57}TiO_3$, may give the highest lithium ionic conductivity, which is generally on the orders of 10^{-4}-10^{-3} S/cm. However, the performance of $Li_{0.3}La_{0.57}TiO_3$ for lithium ion conduction is largely dependent on the method for synthesis, which affects the $Li_{0.3}La_{0.57}TiO_3$ in terms of its composition, the morphology,

[a] Department of Materials Science and Engineering, University of Washington, Seattle, WA 98195

[b] Nuclear Application Tech. Development Department, Korea Atomic Energy Research Institute, Daejeon, 305-353 Rep. of Korea

* Corresponding author. E-mail: gzcao@u.washington.edu

structure, surface chemistry and crystallinity of individual grains, as well as grain boundaries. In literature, $Li_{0.3}La_{0.57}TiO_3$ has been reported to be synthesized with either a solid state reaction method or a sol-gel based method. However, the solid state reaction method usually requires the use of ball milling,[15, 27-29] i.e., a mechanical way, to achieve better mixing of the starting materials which are in the form of powder containing Li^+, La^{3+} and Ti^{4+}. This, on one hand, makes the material processing time consuming and, on the other hand, is not an effective way to achieve a perfectly homogeneous dispersion of the starting materials, so resulting in the existence of impure $Li_{0.3}La_{0.57}TiO_3$ in the final product. The impure $Li_{0.3}La_{0.57}TiO_3$ has the composition deviating from the stoichiometric one and accordingly yields unsatisfactory reproducibility to the lithium ion conduction performance of the final product.[28, 29] The sol-gel method may solve the homogeneity problem in the solid state reaction method to some extent, but is also unfavorable because of the lack of extensibility of a sol-gel method when considering stringent conditions for the formation of a $Li_{0.3}La_{0.57}TiO_3$ sol and the need of using rare or expensive chemicals, which serve as solvent and/or surfactant to form and stabilize the sol, leading to a high cost in material synthesis.[30-33] Herein, we report a facile method, i.e., the so-called coagulated solution method in this paper, for the fabrication of $Li_{0.3}La_{0.57}TiO_3$. This method is relatively simple, low-cost, solution-based, and can produce a precursor powder containing the starting materials Li, La and Ti (or TiO_2) efficiently with good homogeneity, thus to a large extent overcoming the drawbacks of the solid state reaction method in the difficulty of getting ideally mixed starting materials and the sol gel method being complicated with high costs. The $Li_{0.3}La_{0.57}TiO_3$ synthesized resulting from our method demonstrates a decent lithium ionic conductivity on the order of 10^{-4} S/cm for single crystalline grains of the lithium lanthanum titanate and an overall conductivity on the order of 10^{-5} S/cm; the latter counts the hindrance of grain boundaries to the lithium ion conduction in view of polycrystalline structure of the bulk lithium lanthanum titanate material. Such an overall conductivity on the order of 10^{-5} S/cm is comparable to or at a slightly higher level compared with the values in literature for the $Li_{0.3}La_{0.57}TiO_3$ synthesized with a solid state reaction method or a sol-gel method, which varies in a wide range, from 10^{-6} S/cm to 10^{-4} S/cm, relying on the material microstructure, processing parameters, and measurement conditions.[29, 34-36]

In a typical synthesis, 0.02 mol of lithium acetate dehydrate ($LiAc \cdot 2H_2O$) was firstly dissolved in 200 mL of acetic acid (HAc). After the $LiAc \cdot 2H_2O$ has been dissolved completely, 0.067 mol of TiO_2 in the form of nanoparticle powder (P25, commercial TiO_2 nanoparticles, SigmaAldrich) was added, and then the as-obtained mixture was stirred for several hours to get the TiO_2 nanoparticles fully dispersed, resulting in the formation of an uniform dispersion of TiO_2 nanoparticles in HAc containing $LiAc \cdot 2H_2O$. 0.0385 mol of lanthanum acetate
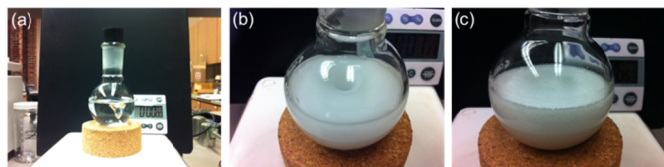

Fig. 1 A record of the transition of a dispersion containing $LiAc \cdot 2H_2O$, $LaAc_3 \cdot 1.5H_2O$, and TiO_2 nanoparticles in HAc from a liquid to a coagulated solution. (a) A clear solution of $LiAc \cdot 2H_2O$ in HAc, (b) TiO_2 nanoparticles and $LaAc_3 \cdot 1.5H_2O$ were added to the solution of $LiAc \cdot 2H_2O$ in HAc, and (c) a coagulated solution forms after being stirred for ~20 min.
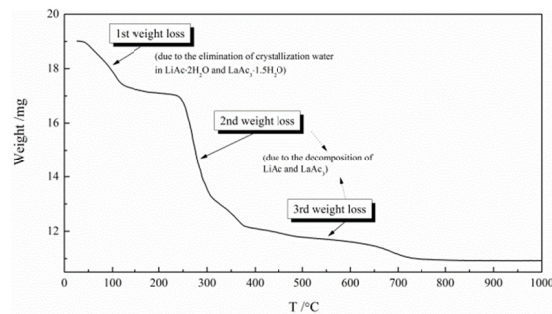

Fig. 2 TGA plot of the precursor powder that contains $LiAc \cdot 2H_2O$, $LaAc_3 \cdot 1.5H_2O$, and TiO_2 used for the synthesis of lithium lanthanum titanate in this work.

hydrate ($LaAc_3 \cdot 1.5H_2O$) was then added to this dispersion. After approximately 20 min into the reaction with vigorous stirring, the liquid dispersion turned to a white coagulated solution, making the formation of a quasi-solid system which consists of Li^+, La^{3+}, and TiO_2 nanoparticles dispersed homogenously. The molar amounts adopted here for $LiAc \cdot 2H_2O$, $LaAc_3 \cdot 1.5H_2O$, and TiO_2 are to obtain $Li_{0.3}La_{0.57}TiO_3$ with stoichiometric ratios, i.e., Li:La:Ti:O=0.3:0.57:1:2. Fig. 1 shows a progression of the transition of the liquid dispersion to a coagulated solution as the $LiAc \cdot 2H_2O$, TiO_2 nanoparticles and $LaAc_3 \cdot 1.5H_2O$ were sequentially added into the HAc solvent. The coagulated solution was then subjected to freeze drying to remove the HAc solvent, resulting in the formation of a dry precursor powder which contains all necessary components: Li^+, La^{3+}, and TiO_2 for the synthesis of lithium lanthanum titanate. Note that the conversion of the liquid precursor into a coagulated solution is a key feature of our method, which makes the positions of the Li^+, La^{3+}, and TiO_2 spatially fixed during the consequential freeze drying treatment and as a result the distribution of all component elements remains highly homogenous when the dry precursor powder forms. It is anticipated that a homogenous component element distribution may facilitate achieving high quality $Li_{0.3}La_{0.57}TiO_3$ by avoiding local composition deviations from the stoichiometry. The formation of a coagulated solution is speculated to originate from the common ion effect[37] in view of the fact that acetic acid was used as solvent for the dissolution of $LaAc_3 \cdot 1.5H_2O$ and $LiAc \cdot 2H_2O$, but the specific mechanism in regard of such an experimental observation still needs to be explored further.
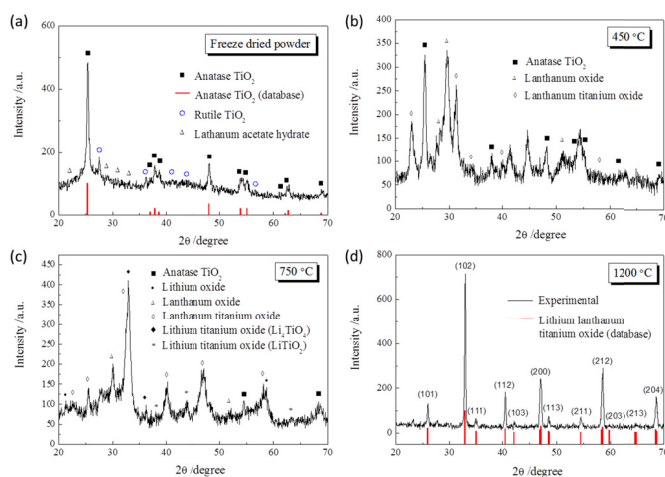

Fig. 3 XRD patterns of (a) freeze dried powder, and (b) through (d) powder annealed at 450 °C, 750 °C, and 1200 °C, respectively.

Before being made into pellets, the freeze dried precursor powder was pre-treated by heating at 750 °C with the aim to get rid of the crystallization water from the $LiAc \cdot 2H_2O$ and $LaAc_3 \cdot 1.5H_2O$ and also get the lithium and lanthanum acetates to further decompose to oxides, so as to avoid a big volume change when the pellets were sintered. The reason of adopting 750 °C is based on the thermal gravimetric analysis (TGA) as shown in Fig. 2, from which it can be seen that the elimination of crystallization water occurs at the temperature around 100 °C, corresponding to the 1st weight loss, and the decomposition of lithium and lanthanum acetates takes place in the temperature range from ~250 °C to ~700 °C, resulting in the 2nd and 3rd weight losses.

Shown in Fig. 3 are XRD patterns of the freeze dried powder (Fig. 3a) and the powder annealed at elevated temperatures (Figs. 3b through 3d), exhibiting a composition evolution of the precursor powder from a mixture of $LiAc \cdot 2H_2O$, $LaAc_3 \cdot 1.5H_2O$, and TiO_2 to pure phase lithium lanthanum titanate with increasing temperature. It can be seen from Fig. 3(b) that the sample annealed at 450 °C presents strong peaks arising from lanthanum oxide and lanthanum titanium oxide, indicating the completed decomposition of lanthanum acetate and the emergence of a compound reaction between the titanium and lanthanum oxides at this temperature level. It also reveals that the 2nd weight loss in the TGA plot (shown in Fig. 2) is due primarily to the decomposition of lanthanum acetate. The decomposition of lithium acetate occurs at relatively high temperature as evidenced by the XRD analysis shown in Fig. 3(c), which corresponds to the sample annealed at 750 °C and presents the peaks of lithium oxide and lithium titanium oxides in addition to those of lanthanum oxide and lanthanum titanium oxide. Considering both the XRD and TGA results, it is clear that a major weight loss of the precursor powder mainly involving the decomposition of lithium and lanthanum acetates takes place when the annealing temperature reaches 750 °C. This confirms the rationality of the 750 °C temperature adopted for the pre-heat treatment of the precursor powder prior to making the pellets. Note that such a pre-heat treatment to the precursor powder with the use of appropriate temperature is a critical step to avoid the pellets from collapse as a result of too big volume change during the sintering. From the XRD pattern shown in Fig. 3d, it can be seen that, when being annealed at 1200 °C, the precursor material converts to

Table 1. A summary of grain conductivity and overall conductivity of the $Li_{0.3}La_{0.57}TiO_3$ sintered at 1000, 1100, 1200 and 1300 °C.

Sample No.	Sintering temperature	Grain conductivity (S/cm)	Overall conductivity (S/cm)
1	1000 °C	4.75×10^{-5}	1.06×10^{-7}
2	1100 °C	2.96×10^{-4}	2.30×10^{-6}
3	1200 °C	3.03×10^{-4}	8.52×10^{-6}
4	1300 °C	3.67×10^{-4}	1.52×10^{-5}

nearly pure phase lithium lanthanum titanate, implying that the as-described coagulated solution method is an effective way to synthesize ternary oxides with well-controlled stoichiometric ratio.

The performance of the prepared $Li_{0.3}La_{0.57}TiO_3$ for lithium ion conduction was studied by measuring the impedance spectra of pellets made of the precursor powder pre-heated at 750 °C in the frequency range from 0.01 Hz to 1 MHz using an impedance analyzer (Model: Solartron 1260/1287) with 10 mV ac amplitude at room temperature. The pellets were prepared with a cold pressing method at 130 MPa pressure and were then sintered at certain temperatures for 6 h in air. A Ti film ~100 nm in thickness was deposited on both sides of the pellets to function as blocking electrodes for lithium ionic conductivity measurement. Shown in Figure 4 are impedance spectra of the $Li_{0.3}La_{0.57}TiO_3$ samples sintered at 1000, 1100, 1200 and 1300 °C. Table 1 summarizes the gain ionic conductivity and overall ionic conductivity of these four samples, which are obtained by fitting the measured impedance plots using the equivalent circuit shown in the inset of Figure 4a. In the equivalent circuit, R_g and R_{gb} represent the resistance corresponding to the ion conduction inside the grains and the resistance arising from the ion conduction at grain boundaries, respectively.[38-45] The lithium ionic conductivity, σ, was calculated using the formula $\sigma = d/(A \cdot R)$, where d is the pellet thickness, A is the area of metal electrodes, and R is the value of resistance obtained from fitting the impedance spectrum. The grain conductivity and overall conductivity were calculated though using the grain resistance, R_g, and the overall resistance, $R_g + R_{gb}$, respectively.

From the results listed in Table 1, one can see that the grain conductivity is on the order of 10^{-5} S/cm for the sample sintered at 1000 °C, and it increases by more than six times to the order of 10^{-4} S/cm when the sintering temperature reaches 1100 °C, implying the formation of pure phase lithium lanthanum titanate approximately at this temperature. A further increase of the sintering temperature to even 1300 °C shows no significant contribution to improving the grain conductivity. As for the overall conductivity, a considerable increase of the overall conductivity from 1.06×10^{-7} S/cm to 2.30×10^{-6} S/cm is observed when the sintering temperature increases from 1000 °C to 1100 °C. This can be attributed to an increase in grain size and improved connection between individual grains due to the melt of material at elevated temperatures, being consistent with the SEM images shown in Figure 5, which reveals that (1) the grains grow from ~500-800 nm (Fig. 5a) to averagely 2 μm (Fig. 5b) as the sintering temperature increases from 1000 °C to 1100 °C, and (2) the voids existing between the grains are largely reduced in view of the melt of the material at the temperature around 1100 °C. As the sintering temperature increases from 1100 °C to 1200 °C, and then to 1300 °C, the overall conductivity displays a gradual increase, from 2.30×10^{-6} S/cm to 8.52×10^{-6} S/cm and 1.52×10^{-5} S/cm, respectively. The increase in the overall conductivity with increasing sintering temperature results from the continued growth of the grains,
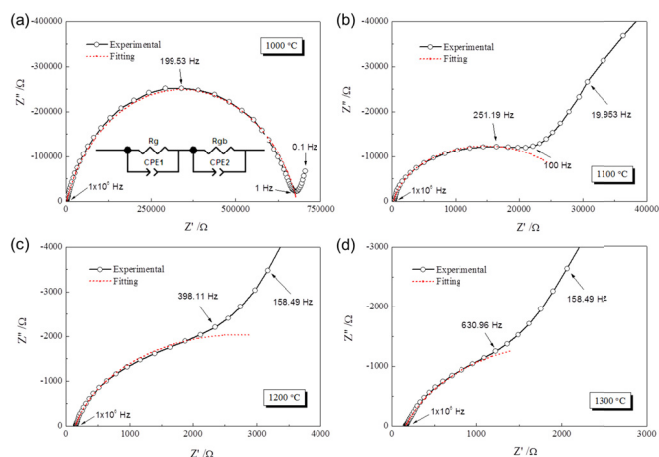

Fig. 4 Impedance spectra of $Li_{0.3}La_{0.57}TiO_3$ sintered at (a) 1000 °C, (b) 1100 °C, (c) 1200 °C, and (d) 1300 °C marked with representative values of the applied frequency. The inset of (a) depicts the equivalent circuit employed for fitting the impedance spectra. (R_g: grain resistance, R_{gb}: grain boundary resistance, CPE: constant phase element.)
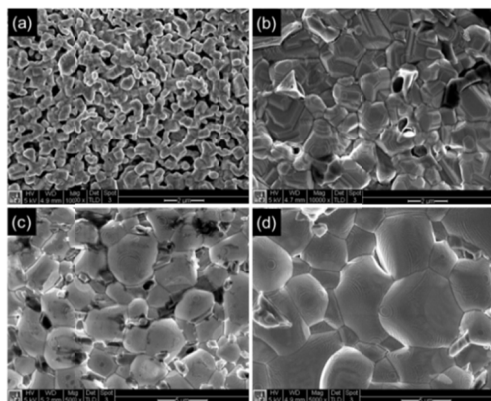
Fig. 5 SEM images of the $Li_{0.3}La_{0.57}TiO_3$ pellet samples sintered at (a) 1000 °C, (b) 1100 °C, (c) 1200 °C, and (d) 1300 °C. (Scale bar: 2 μm for (a) and (b), 5 μm for (c) and (d))

from ~2 μm for 1100 °C to larger than 5 μm for 1300 °C, and a further decrease of grain boundaries, evidenced by Figs. 5b through 5d. These results, i.e., the grain conductivity on the order of 10^{-4} S/cm and the overall conductivity on the order of 10^{-5} S/cm for pellet sample sintered at 1300 °C, are comparable to most of the values and are slightly higher than some of the values of conductivities reported in literature for the $Li_{0.3}La_{0.57}TiO_3$ synthesized with traditional solid state reaction method[16, 18, 27, 35, 46, 47] or sol-gel method,[31, 32, 48, 49] which are typically on the orders of 10^{-4}-10^{-3} S/cm for the grain conductivity and on the orders of 10^{-6}-10^{-5} S/cm for the overall conductivity (- Note that in some reports a temperature even higher than 1300 °C was adopted for sintering). While the achieved conductivities are at the same level, compared with the traditional methods, our coagulated solution method in term of material synthesis is however much simpler and highly efficient.

In summary, the coagulated solution method involving dissolving lithium acetate and lithium lanthanum and dispersing commercial TiO_2 nanoparticles in acetic acid has proven to be an effective approach for the preparation of $Li_{0.3}La_{0.57}TiO_3$ precursor powder, which gives rise to a highly homogeneous distribution of the component elements through a simple, scalable, and reproducible way. The lithium ionic conductivities of $Li_{0.3}La_{0.57}TiO_3$ produced with this method are on the order of 10^{-4} S/cm for single crystalline grains and 10^{-5} S/cm for the bulk material. The conductivities are comparable to the values reported in literature for the material synthesized with a solid state reaction or sol-gel method. In addition to the synthesis of $Li_{0.3}La_{0.57}TiO_3$, the coagulated solution method is also thought of an extendable approach for the fabrication of other multi-element oxides with the capability to easily and consistently control the stoichiometric composition of the material.

Notes and references

1. D. Doughty and E. Peter Roth, *Interface-Electrochemical Society*, 2012, **21**, 37.
2. M. Park, X. Zhang, M. Chung, G. B. Less and A. M. Sastry, *Journal of Power Sources*, 2010, **195**, 7904-7929.
3. D. Aurbach, E. Zinigrad, Y. Cohen and H. Teller, *Solid State Ionics*, 2002, **148**, 405-416.
4. N. Williard, W. He, C. Hendricks and M. Pecht, *Energies*, 2013, **6**, 4682-4695.
5. M. Yoshio, R. J. Brodd and A. Kozawa, *Lithium-ion batteries: science and technologies*, Springer, 2009.
6. J. Christensen, P. Albertus, R. S. Sanchez-Carrera, T. Lohmann, B. Kozinsky, R. Liedtke, J. Ahmed and A. Kojic, *Journal of The Electrochemical Society*, 2012, **159**, R1-R30.
7. G. Girishkumar, B. McCloskey, A. Luntz, S. Swanson and W. Wilcke, *The Journal of Physical Chemistry Letters*, 2010, **1**, 2193-2203.
8. M. Ogawa, K. Yoshida and K. Harada, *SEI Technical Review*, 2012, 88-90.
9. M. Yang and J. Hou, *Membranes*, 2012, **2**, 367-383.
10. V. Thangadurai and W. Weppner, *Ionics*, 2006, **12**, 81-92.
11. A. Manuel Stephan, *European Polymer Journal*, 2006, **42**, 21-42.
12. F. Croce, G. Appetecchi, L. Persi and B. Scrosati, *Nature*, 1998, **394**, 456-458.
13. N. Kamaya, K. Homma, Y. Yamakawa, M. Hirayama, R. Kanno, M. Yonemura, T. Kamiyama, Y. Kato, S. Hama and K. Kawamoto, *Nature materials*, 2011, **10**, 682-686.
14. X.-W. Zhang, C. Wang, A. J. Appleby and F. E. Little, *Journal of Power Sources*, 2002, **112**, 209-215.
15. J. Emery, J. Buzare, O. Bohnke and J. Fourquet, *Solid State Ionics*, 1997, **99**, 41-51.
16. Y. Inaguma, J. Yu, T. Katsumata and M. Itoh, *Nippon seramikkusu kyokai gakujutsu ronbunshi*, 1997, **105**, 548-550.
17. S. Stramare, V. Thangadurai and W. Weppner, *Chemistry of materials*, 2003, **15**, 3974-3990.
18. K.-Y. Yang, J.-W. Wang and K.-Z. Fung, *Journal of Alloys and Compounds*, 2008, **458**, 415-424.
19. S. Duluard, A. Paillassa, L. Puech, P. Vinatier, V. Turq, P. Rozier, P. Lenormand, P.-L. Taberna, P. Simon and F. Ansart, *Journal of the European Ceramic Society*, 2013, **33**, 1145–1153.
20. M. Kotobuki, K. Hoshina, Y. Isshiki and K. Kanamura, *Phosphorus Research Bulletin*, 2011, **25**, 61-63.
21. D. Popovici, H. Nagai, S. Fujishima and J. Akedo, *Journal of the American Ceramic Society*, 2011, **94**, 3847-3850.
22. E. J. Cussen, *Journal of Materials Chemistry*, 2010, **20**, 5167-5173.
23. V. Thangadurai, H. Kaack and W. J. Weppner, *Journal of the American Ceramic Society*, 2003, **86**, 437-440.
24. V. Thangadurai and W. Weppner, *Advanced Functional Materials*, 2005, **15**, 107-112.
25. A. Hayashi and M. Tatsumisago, *Electronic Materials Letters*, 2012, **8**, 199-207.
26. A. Sakuda, A. Hayashi and M. Tatsumisago, *Scientific reports*, 2013, **3**, 2261.
27. C. W. Ban and G. M. Choi, *Solid State Ionics*, 2001, **140**, 285-292.
28. K. Kishida, M. Miyata, N. Wada, N. L. Okamoto, K. Tanaka, H. Inui, H. Koyama, T. Hattori, Y. Iriyama and Z. Ogumi, *Journal of electron microscopy*, 2007, **56**, 225-234.
29. L. Sun, K. Sun and S. Dillon, *Proc. of SPIE*, 2011, **8035**, 803508.
30. H. Geng, A. Mei, Y. Lin and C. Nan, *Materials Science and Engineering: B*, 2009, **164**, 91-95.
31. H. X. Geng, J. L. Lan, A. Mel, Y. H. Lin and C. W. Nan, *Electrochim. Acta*, 2011, **56**, 3406-3414.
32. T. N. H. Le, M. Roffat, Q. N. Pham, S. Kodjikian, O. Bohnke and C. Bohnke, *J. Sol-Gel Sci. Technol.*, 2008, **46**, 137-145.
33. I. C. Popovici, E. Chirila, V. Popescu, V. Ciupina and G. Prodan, *Journal of materials science*, 2007, **42**, 3373-3377.
34. H. Geng, A. Mei, C. Dong, Y. Lin and C. Nan, *Journal of Alloys and Compounds*, 2009, **481**, 555-558.
35. Y. Inaguma, C. Liquan, M. Itoh, T. Nakamura, T. Uchida, H. Ikuta and M. Wakihara, *Solid State Communications*, 1993, **86**, 689-693.
36. J. Wolfenstine, J. Allen, J. Read, J. Sakamoto and G. Gonalez-Doncel, *Journal of Power Sources*, 2010, **195**, 4124-4128.
37. R. H. Petrucci, W. S. Harwood, G. Herring and J. Madura, *General chemistry: principles and modern applications*, Prentice Hall Upper Saddle River, NJ, 1997.
38. A. e. A. Saif and P. Poopalan, *Physica B: Condensed Matter*, 2011, **406**, 1283-1288.
39. Z. V. Mocanu, G. Apachitei, L. Padurariu, F. Tudorache, L. P. Curecheriu and L. Mitoseriu, *European Physical Journal-Applied Physics*, 2011, **56**, 132.
40. J.-M. Winand and J. Depireux, *EPL (Europhysics Letters)*, 1989, **8**, 447.
41. S.-i. Furusawa, *Physics of Solid State Ionics*, 2006, 271-302.
42. M. Kotobuki, in *2nd International Conference on Electrical, Electronics and Civil Engineering (ICEECE'2012)*, Singapore, 2012, pp. 165-167.
43. M. Kotobuki, K. Kanamura, Y. Sato, K. Yamamoto and T. Yoshida, *Journal of Power Sources*, 2012, **199**, 346-349.
44. M. Kotobuki, K. Kanamura, Y. Sato and T. Yoshida, *Journal of Power Sources*, 2011, **196**, 7750-7754.
45. O. Bohnke, S. Ronchetti and D. Mazza, *Solid State Ionics*, 1999, **122**, 127-136.
46. L. Sun, K. Sun and S. Dillon, in *Proc. of SPIE*, International Society for Optics and Photonics, 2011, pp. 803508-803501-803508.
47. C. H. Chen and K. Amine, *Solid State Ionics*, 2001, **144**, 51-57.
48. K. Dokko, N. Akutagawa, Y. Isshiki, K. Hoshina and K. Kanamura, *Solid State Ionics*, 2005, **176**, 2345-2348.
49. S. Suda, H. Ishii and K. Kanamura, in *Materials Research Society Symposium Proceedings*, Cambridge Univ Press, 2003, pp. 57-62.

ChemComm Accepted Manuscript